Effects of Anions on the NMR Relaxation of Pyridinium and Di-*tert*-Butylpyridinium Ions in Acid Solution. Implications for Chemisorption on Solid Acids

Dan Fărcaşiu,* Marta Lezcano, and Povilas Lukinskas

Department of Chemical and Petroleum Engineering, University of Pittsburgh, 1249 Benedum Hall, Pittsburgh, Pennsylvania 15261

David H. Waldeck[1]

Department of Chemistry, University of Pittsburgh, Chevron Science Center, Pittsburgh, Pennsylvania 15260

Received: December 23, 1999; In Final Form: April 4, 2000

The line shape of the NMR signals of protons bonded to nitrogen shows that the longitudinal relaxation of ^{14}N (T_{1N}) is much faster for di-*tert*-butylpyridinium ions ($DTBPH^+$) than for pyridinium (PyH^+) in solution. The relaxation times for ring carbons (T_{1C}) indicate that the difference comes from a different rate of tumbling in solution, rather than from a difference in the electric field gradient. Computer modeling gives ratios of relaxation times ($T_{1N} = 1/R_{1N}$) of 10−20. Ion pairing has an opposite effect upon the two ions: it accelerates the relaxation of PyH^+ but slows down the relaxation of $DTBPH^+$. In the absence of electrostatic interactions with the solvent, ion pairing should increase the correlation time τ_c (decrease T_1) for the anion positioned in the plane of the ring and should have only a small effect on τ_c for the anion perpendicular to the ring (along the *z* axis). The anion in the ion pair of PyH^+ is positioned on the *x* axis (the C_2 axis of the ring) for maximum hydrogen bonding with the N−H group. The inability of DTBP to form hydrogen bonds at nitrogen was confirmed by the equality of its ^{15}N chemical shifts in methyl *tert*-butyl ether, dry and containing water. B3LYP/6-31G* calculations indicate that the positioning of an anion along the *z* axis of $DTBPH^+$ induces a charge redistribution that reduces the electrostatic interaction of the cation with the solvent dipoles in the *xy* plane, thus decreasing the tumbling correlation time, τ_c, and increasing the NMR relaxation time, T_1. These data suggest that chemisorption of pyridine on acid sites on solid surfaces occurs with the nitrogen facing the surface but that DTBP is chemisorbed on the side (flatwise) with its degree of hydronation depending on the degree of curvature of the surface around the site.

Introduction

Pyridine has been extensively used as a probe base for the characterization of acid sites on solid catalysts.[2] The methods of analysis employed have included IR spectroscopy;[3] microcalorimetry;[4] proton,[5] carbon,[6] and nitrogen NMR;[7] and temperature-programmed desorption.[8] The use of the thermal methods, however, has been criticized.[9] Because pyridine reacts with both Lewis and Brønsted acid sites, 2,6-dimethylpyridine (DMP) has been proposed for use in targeting specifically the Brønsted sites.[10] Other workers, however, reported IR bands assigned to complexes of DMP with Lewis acid sites on various solids.[11] The sterically hindered 2,6-di-*tert*-butylpyridine has been proposed for use in distinguishing the sites on the external surface of solids[10,12] from those inside pores.[13]

Differences between the interactions of pyridine (Py, **1**) and 2,6-di-*tert*-butylpyridine (DTBP, **2**) with acid sites on solid surfaces are likely. (See Chart 1.) It is known that ionic reactions on solid surfaces involve tight ion pairs as intermediates and that separation of the ions does not occur.[14] The steric bulk of **2** is expected to reduce its ability to form ion pairs. Because the physisorption of pyridine through hydrogen bonding orients the ring with the N···C4 axis (the C_2 axis) perpendicular to the surface,[15] the same orientation should be preferred, if not required, in the ion pair of the pyridinium cation ($Py-H^+$, **3**) formed by chemisorption. The voluminous substituents of **2** hold the nitrogen atom farther away from the surface.

CHART 1

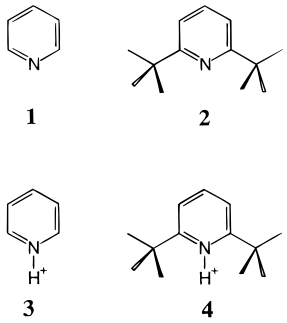

1 **2** **3** **4**

As an additional factor, it has been determined that the pK_b of **2** *in solution* is abnormally low, particularly in comparison with those of the lower 2,6-dialkylpyridine homologues and with the relative basicities in the gas phase.[16] This anomaly was rationalized by steric hindrance, which prevents the hydrogenated DTBP from forming a hydrogen bond with the anion,[16a,b] or by the steric inhibition of cation solvation.[16a,b,17] The analysis was complicated, however, by a study that concluded that both **2** and the corresponding cation ($DTBH^+$, **4**) are hydrogen-bonded at nitrogen in water.[18] The reduced basicity was assigned

* Author to whom correspondence should be addressed. Telephone: 412-624-7449. Fax: 412-624-9639. E-mail: dfarca@pitt.edu.

10.1021/jp994472f CCC: $19.00
Published on Web 05/10/2000

to a decrease in entropy because of an increased barrier to *tert*-butyl group rotation.[18] To further the controversy, it was concluded from an IR spectroscopic investigation that 4-fluorophenol forms hydrogen bonds with the π-electron system of DTBP, rather than with the nitrogen atom,[19] whereas it was concluded from another study that, despite the steric hindrance, DTBP interacts not only with Brønsted acid sites, but also with Lewis acid sites on the surface of boron phosphate.[12d]

Because all of the previous studies were based on an examination of changes in the spectra of the hydrogen-bond donors, we determined the solvent effects on the ^{15}N NMR chemical shifts of **2**. There was no dependence of chemical shifts on the hydrogen-bond donor ability of solvents, in stark contrast to the behavior of **1**.[20] We can, therefore, expect differences in the interactions of **1** and **2** with external acid sites. In particular, not all of the sites that react with pyridine should be expected to react with 2,6-di-*tert*-butylpyridine.

In continuation of our studies of probe bases for acidity measurements of solid and liquid acids,[14d] we examined the hydronation of **1** and **2** in acids of varying strength, by ^{1}H, ^{13}C, and ^{15}N NMR spectroscopy. The study has yielded results on the NMR relaxation of the hydronated bases, which are significant for understanding their interactions with anions in solution and with anionic sites on solids. We report our results in full here.

Methods

NMR Experiments. All reagents and solvents were reagent grade and were used as purchased. The NMR spectra[9a] were recorded at 300.13 MHZ for ^{1}H, 75.468 MHZ for ^{13}C, and 30.424 MHZ for ^{15}N. Each acid solution was prepared by weighing the components on an analytical balance (0.1 mg accuracy) to give a 1.5 M solution of base in acid in the 8-mm NMR tube. External cooling was applied during mixing. The sample of pyridine in trifluoromethanesulfonic acid (TFMSA) was prepared by freezing pyridine in the NMR tube in liquid nitrogen, adding less than the total calculated amount of TFMSA, then bringing the mixture to room temperature and adding the rest of the exact weight of acid required. After the solution was prepared, each tube was tightly capped and placed in a thin-walled 10-mm OD NMR tube containing the lock solvent and the chemical shift reference compound, which was $CDCl_3$ with 1% TMS for the ^{1}H and ^{13}C spectra and an 80:20 Py/DMSO-d_6 mixture for the ^{15}N spectra. The ^{1}H NMR chemical shifts were then recalibrated from internal dichloroethane (δ 3.72 ppm), as described previously.[20] "Room temperature" was the normal probe temperature, 22 °C.

Computations. The ab initio calculations were performed with the Gaussian 98 programs.[21] The charge distributions were obtained by Mulliken population analyses on structures optimized by density functional theory (DFT)[22] at the B3LYP/6-31G* level.[23]

Hydrodynamic calculations of the rotational relaxation times were conducted in the manner described previously.[24] The dimensions of the cations were obtained from B3LYP/631G* calculations. For the ion pairs with the anion on the side, the trifluoroacetate anion was placed with the C−C bond on the *x* (C_2) axis and with the oxygen atoms at equal distances (1.7 Å) from the hydrogen bonded to the nitrogen atom. For the ion pair with the anion on the top, the trifluoroacetate was likewise placed along the *z* axis (perpendicular to the plane of the ring) and with the oxygen atoms at a distance of 4.00 Å from the ring.

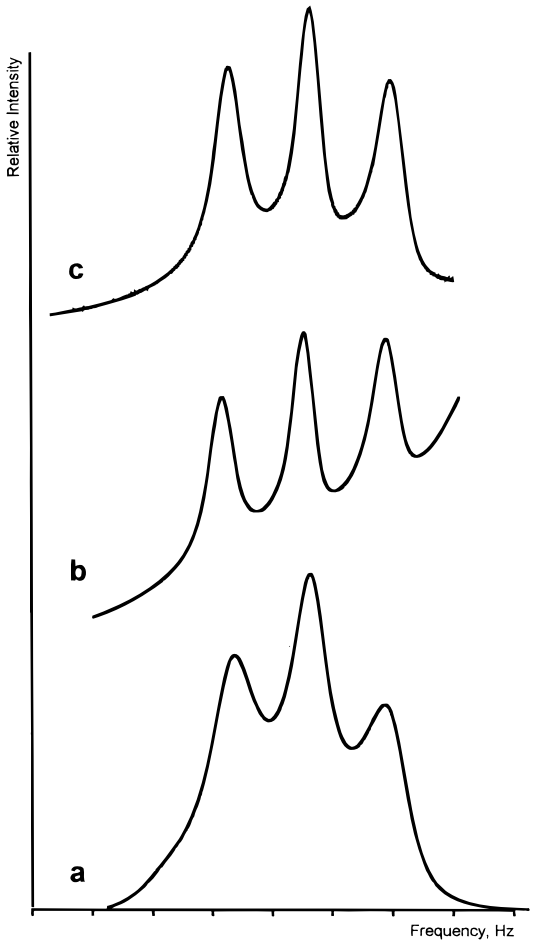

Figure 1. NMR signal of the proton bonded to nitrogen in PyH^+ (frequency scale: 50 Hz/division). (a) Trifluoroacetate anion, trifluoroacetic acid solution; (b) trifluoromethanesulfonate anion, trifluoromethanesulfonic acid solution; and (c) trifluoromethanesulfonate anion, trifluoroacetic acid solution.

The simulated curves in the figures were generated with the computer program SigmaPlot, developed by Jandel Scientific.[25]

Results and Discussion

The proton NMR spectrum of the conjugate acid of Py ($Py-H^+$, **3**) in trifluoroacetic acid (TFA) was first reported in a study that exploited the triplet for the $N-H^+$ resonance to measure chemical shifts (in that case of ^{14}N) by double resonance.[27] We also observed a triplet for the $N-H^+$ signal of **3**, at δ 13.96 ppm in TFA and at δ 12.70 ppm in trifluoromethanesulfonic acid (TFMSA), as shown in Figure 1. The acid protons (OH) resonated at 12.21 and 11.99 ppm, respectively. The chemical shifts measured from an internal reference (see the Methods section) are somewhat different from the values based on an external reference, reported earlier.[26] Because of the much higher field, the NH and OH signals in TFA solution were much better separated in our experiments than in the pioneering work of Baldeschweiler and Randall,[27] but for the TFMSA solution, the $N-H^+$ resonance was riding on the tail of the TFMSA proton's peak. We also examined a sample of $PyH^+ \cdot TFMSA^-$ in TFA solution (Figure 1c), which gave a triplet for δ(NH) that was well separated from the acid peak.

The one-bond coupling constants that we measured were somewhat different in different media: 62.5 Hz in TFA, 68.3 Hz in TFMSA, and 67.3 Hz for $PyH^+ \cdot TFMSA^-$ in TFA. These are absolute values; the sign of *J* was not determined. The

TABLE 1: ^{1}H NMR Spectral Data for the Di-*tert*-butylpyridinium Ion[a]

proton	N−H	β	γ	Me
chemical shift (δ, ppm)[b]	11.28	7.98	8.55	1.59
coupling constants (Hz)	1.7 ± 0.2[c]	8.0 ± 0.2[d]	8.0 ± 0.2[d]	
	91.4 ± 0.7[e]	1.7 ± 0.2[c]		
		4.0 ± 0.2[f]		

[a] In TFMSA, from 1,2-dichloroethane (δ 3.72) as internal standard. [b] The values in TFA are 11.17, 7.93, 8.48, and 1.59 ppm, respectively. [c] J(H−Cβ−N−H), measured on the β hydrogen signal (see text). [d] J(H−Cβ−Cγ−H). [e] $|J|$(^{15}N−H), measured in the ^{15}N spectrum. [f] $|J|$(^{15}N−Cα−Cβ−H), measured in the ^{15}N spectrum.

variations in $|J|$(^{14}N−H) are in line with literature reports, which give J(^{15}N−H) = −96.3 Hz for the PyH$^+$·TFA$^-$ in TFA solution,[28] $|J|$(^{15}N−H) = 83−89 Hz for the hydrochloride in $CDClF_2/CDF_3$ between 168 and 112 K,[29] and $|J|$(^{15}N−H) = 88−91 Hz for the nitrate in $CDClF_2/CDF_3$ between 144 and 112 K.[29] Conversion of these published values with the equation: J(^{15}N−H) = 1.4027J(^{14}N−H),[30] gave values for $|J|$(^{14}N−H) of 68.6, 59.2−63.4, and 62.7−64.8 Hz, respectively. Theoretical calculations indicate that the coupling constants increase with the dielectric constant of the medium,[31a] but the values measured for J(^{15}N−H) of methylacetamide, −92.9 Hz in tetrachloromethane and − 93.0 Hz in water, seem too close to each other to account for the differences cited above.[31b]

In contrast, we observed a broad singlet at δ 11.17 in the spectrum of 2,6-di-*tert*-butylpyridine in TFA (Table 1 and Figure 2a), well separated from the acid peak at δ 12.65. The same line shapes and chemical shifts were observed for the corresponding signals in the ^{2}H NMR spectrum of DTBP in TFA-*d*. The chemical shifts in TFMSA were 11.28 (br s, NH, Figure 2b) and 12.53 (OH). The ^{15}N NMR chemical shifts were −185.78 in TFA and −185.76 in TFMSA (lower frequency from external, neat nitromethane), thus showing that hydronation was complete in both acids (DTBH$^+$, **4**).

Several lines of evidence indicated that the shape of the NH signal of **4** did not result from chemical exchange.[32] First, Gold and Lee established that the sterically hindered chemical exchange of DTBPH$^+$ is much slower than that of PyH$^+$.[32c] Second, we found that the NH singlet sharpened[33] instead of broadening[32c] upon cooling from 22 to 0 and then to −20 °C. Third, the fully coupled ^{15}N spectrum showed a doublet of triplets, with the large splitting giving $|J|$(^{15}N−H) = 91.4 ± 0.7 Hz (three determinations) and the triplet splitting giving $|J|$(^{15}N−Cα−Cβ−H) = 4 ± 0.2 Hz. Likewise, the signal for the β hydrogens was, in our spectra, a doublet of doublets, with J(H−Cβ−Cγ−H) = 8 ± 0.2 Hz and J(H−Cβ−N−H) = 1.7 ± 0.2 Hz (Table 1). The closer doublets collapsed upon irradiation of the N−H signal. The small H−Cβ−N−H signal would be the first eliminated by the exchange of the N−H proton.

On the other hand, some of the broadening of the bands of the N−H triplet of **3** in TFMSA *did* result from chemical exchange. The signals of the protons bonded to the carbons in **3** were somewhat broad, but we could ascertain that the peak of the protons in the β positions was not split by coupling with the proton bonded to the nitrogen atom, as it was in the spectrum of **4**, because irradiation at the center of the N−H resonance failed to produce any narrowing of the β-hydrogen triplet (overall half-line widths of 16.6 and 16.5 Hz for the two experiments). The line width of the acid peak was about 2.7 Hz in both cases. A further analysis of the spectrum was rendered difficult by the overlap of the signals for the α and γ protons, but irradiation at the N−H resonance altered the overall

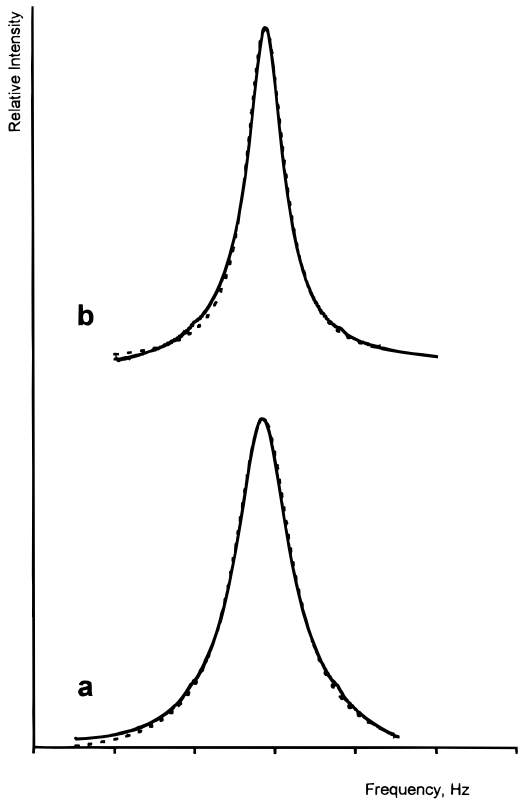

Figure 2. NMR signal of the proton bonded to nitrogen in DTBPH$^+$ (frequency scale: 50 Hz/division) (a) Trifluoroacetate anion, trifluoroacetic acid solution (—, experimental; ···, calculated for η = 2.49) and (b) trifluoromethanesulfonate anion, trifluoromethanesulfonic acid solution (—, experimental; ···, calculated for η = 1.46).

shape of the composite signal for Hα and Hγ and reduced its width, indicating some coupling of the N−H and the α protons. Also, irradiation of the composite signal for the α and γ protons narrowed slightly the lines of the N−H triplet. The chemical exchange should be faster in the weaker acid, TFA.[32]

The NMR signals of protons bonded to nitrogen in various compounds have been known to vary, in the absence of chemical exchange, from sharp triplets (e.g., for the ammonium ion in acid solution)[34] to more or less broad singlets (e.g., for pyrrole).[33,35] The reported differences were brought about by changes in the bonding of the nitrogen atom and its ligands and were rationalized by variations in the effectiveness of the electric quadrupole relaxation of the ^{14}N atoms.[33] The difference between the line shapes of the N−H$^+$ signals of **3** and **4** observed by us can also be assigned to the faster electrical quadrupole relaxation of ^{14}N in the latter, caused this time by the introduction of substituents at other sites of the molecule, rather than at nitrogen.

For an infinitely slow relaxation, the signal of the proton bonded to ^{14}N is a 1:1:1 triplet. As the rate of relaxation increases, the triplet is distorted such that the lines are broadened and the central line increases in intensity at the expense of the outer lines until the latter disappear altogether. The resulting broad singlet sharpens upon a further increase in the relaxation rate. Thus, the rate of the electric quadrupole relaxation can be assessed by an analysis of the shape of the signal. For a certain range of relaxation rates, the relaxation times (T_{1N}) can be obtained from the equations developed by Pople (eqs 1−3),[36] which give the relative spectral intensity I as a function of the frequency (distance from the central proton resonance ν_H) and a dimensionless parameter η (in the notation of ref 36a).

$$I(x) = \left[\frac{2\eta}{\pi J(\mathrm{N-H})}\right] \left[\frac{45 + \eta^2(5x^2 + 1)}{225x^2 + \eta^2(34x^4 - 2x^2 + 4) + \eta^4(x^6 - 2x^4 + x^2)}\right] \quad (1)$$

$$\eta = 10\pi T_{1\mathrm{N}} J(\mathrm{N-H}) \quad (2)$$

$$x = \frac{\nu - \nu_{\mathrm{H}}}{J(\mathrm{N-H})} \quad (3)$$

In the range of faster relaxation (the case of **4**), the calculated intensities can be fit to the experimental spectrum by varying the parameter η, as indicated in the Methods section. The simulation gave values for η of 1.46 in TFMSA and 2.49 in TFA (Figure 2). The quality of the spectra, which would affect the line broadening, is similar for the two spectra, as shown by the half-height widths of 1.83 and 2.20 Hz for the *tert*-butyl lines in TFMSA and TFA.

For the spectra of **3**, signal shape fitting was less satisfactory, because of the superimposed effect of chemical exchange. The homodecoupling experiments described above indicate that the effects of the unresolved spin−spin coupling of N−H with the α, β, and γ protons are marginal. It is, therefore, more accurate to compare the calculated and experimental relative intensity of the three bands of the N−H triplet. The chemical exchange broadens the three lines equally and, thus, does not change their relative heights. The center band intensity, I(c), is obtained from eq 1 for $\nu = \nu_{\mathrm{H}}$ ($x = 0$), and the sideband intensity, I(s), is obtained for $\nu - \nu_{\mathrm{H}} = J$(N−H) ($x = 1$). Their ratio is then calculated using eq 4.

$$\frac{I(\mathrm{c})}{I(\mathrm{s})} = \frac{(45 + \eta^2)(75 + 12\eta^2)}{60\eta^2 + 8\eta^4} \quad (4)$$

Typical values are

η	10	20	30	31.62	40	100	∞
I(c)/I(s)	2.15	1.66	1.57	1.566	1.54	1.51	1.50
	100/47	100/60	100/63	100/64	100/65	100/66	100/67

The highest value of η for which the shape of the $I(x)$ function for the ^{14}N−H resonance was calculated in the literature was 31.62 ($\eta^2 = 1000$).[36a,c] In fact, the values beyond that do not give a significant change in the I(c)/I(s) ratio, and at some point, eq 1 itself is no longer valid.[36] It is seen that the predicted limiting value for I(c)/I(s) is 1.5 instead of 1.0. The experimental values for I(c)/I(s) are 100/68 for Py in TFA (**3**·TFA$^-$, Figure 1a) and 100/(79 ± 2) for **3**·TFMSA$^-$ in TFA (Figure 1c). Because the N−H signal of **3**·TFMSA$^-$ in TFMSA (Figure 1b) partially overlapped with the OH signal, only the high-frequency (downfield) sideband could be measured; it gave I(c)/I(s) ≈ 100/80. A comparison with the calculated values shows that, in all three cases, η was outside the limits of applicability of eq 1. We can, therefore, conclude that the values of η for the spectra of **3** were, in all cases, greater than 31.2 and that it was greater for the TFMSA solution than for the TFA solution. We note that **3**·TFMSA$^-$ gave the same I(c)/I(s) value in TFMSA and TFA solutions, which indicates that the counterion has a greater effect on the relaxation rate than the solvent.

The coupling constant $|J|(^{14}\mathrm{N-H})$ for DTBPH$^+$, 65.2 Hz (calculated as 91.4/1.4027, see above), is about the same as the coupling constant $|J|(^{14}\mathrm{N-H})$ for PyH$^+$, for which our measurements give an average value of 66.0 Hz. Therefore, the variation of the η parameter from PyH$^+$ to DTBPH$^+$ reflects entirely the change in the corresponding ^{14}N longitudinal relaxation times.

TABLE 2: NMR Longitudinal Relaxation Times of Carbon Atoms ($T_{1\mathrm{C}}$) in Pyridine, Di-*tert*-butylpyridine, and Their Cations in Various Solvents

		Cα		Cβ		Cγ	
solute	solvent	δ, ppm	T_1, s	δ, ppm	T_1, s	δ, ppm	T_1, s
Py	hexane[b]	150.7	21.1	123.8	22.5	135.5	22.2
	phenol[b]	147.3	1.6	124.7	1.5	137.9	0.44
	TFA[b]	148.3	1.6	128.2	2.9	141.7	2.7
	TFMSA	148.8	3.5	128.4	4.7	141.5	4.8
DTBP	hexane[b]	168.1	37.3	115.7	5.3	136.4	7.0
	phenol[b]	167.6	9.9	*a*	−	136.5	1.31
	TFA[b]	164.2	6.1	122.9	0.79	148.6	1.1
	TFMSA	163.4	5.0	122.6	0.55	147.8	0.79

[a] Covered by the solvent. [b] Viscosities: 0.29 cP, hexane; 7.1 cP, phenol; and 0.75 cP, TFA.

For rapid molecular tumbling and axial symmetry of the molecular electric field, the relaxation time is determined by two variables, the electric field gradient q and the correlation time for tumbling, τ_{c},[37a] as shown in eq 5, where C is a collection of constants.

$$1/T_{1\mathrm{N}} = \mathrm{C}q^2\tau_{\mathrm{c}} \quad (5)$$

As both **3** and **4** fit the definition of "small" molecules (MW < 200 daltons),[37b] they should satisfy eq 6, which is derived from eqs 2 and 5.

$$\frac{\eta(\mathrm{PyH}^+)}{\eta(\mathrm{DTBPH}^+)} = \frac{q^2(\mathrm{DTBPH}^+)\tau_{\mathrm{c}}(\mathrm{DTBPH}^+)}{q^2(\mathrm{PyH}^+)\tau_{\mathrm{c}}(\mathrm{PyH}^+)} \quad (6)$$

In fact, the temperature dependence observed for the line width of **4** (a narrower N−H band at lower temperature) validates the assumption of fast tumbling (extreme narrowing condition).

To help determine which factor controls the relaxation times, we measured[38] the longitudinal relaxation times for the carbon atoms ($T_{1\mathrm{C}}$) of Py and DTBP in various solvents. The results are given in Table 2, and they are accurate to about 10% relative uncertainty. For the acid solutions, it can be seen that the $T_{1\mathrm{C}}$ values of Cβ and Cγ are about the same for both **3** and **4**. Unlike the nitrogen electric quadrupole relaxation time ($T_{1\mathrm{N}}$), the $T_{1\mathrm{C}}$ parameter is not a simple function of τ_{c},[37c] but the similarity of $T_{1\mathrm{C}\beta}$ and $T_{1\mathrm{C}\gamma}$ is important, because it indicates that the variation in the relaxation times is determined by the change in the correlation time for tumbling, τ_{c}, rather than in the electric field gradient.

The relative contribution of the factors of eq 6 was also assessed by calculating, at the B3LYP/6-31G* level, the electrical field gradient at nitrogen for **3**, **4**, and their ion pairs with a model anion (F$^-$) placed on the side (facing the N−H bond) or on the top of the ring. Although the absolute values were large, the differences between the values for **3** and **4** were less than 0.1%. The ion pairing and the change in the position of the anion change the component of the electrical field gradient that is the main component, but the change in value for both the main component and the asymmetry parameter[39] are negligible.

The rate of tumbling in solution is determined by the size of the molecule and the viscosity of the solvent, as shown by comparisons of the $T_{1\mathrm{C}}$ values given in Table 2 for **1** (smaller molecule) and **2** (larger molecule) in hexane (low viscosity) and phenol (high viscosity). The long relaxation times for Cα of **2** are normal for its degree of substitution. It is noteworthy

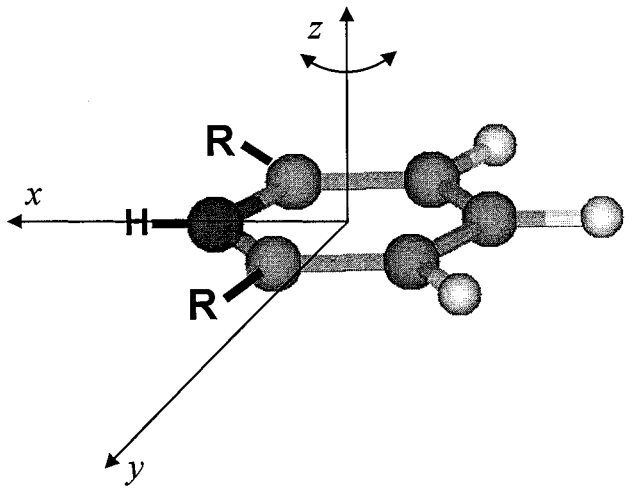

Figure 3. Principal axes for the rotation (tumbling) of cations **3** and **4**.

that the transfer from hexane to phenol has a significantly greater effect on the relaxation of **1** than on the relaxation of **2**, because strong hydrogen bonding, which exists for the former but not for the latter, produces an additional friction.[20] It is interesting, however, that the transfer from TFMSA to TFA has an opposite effect on the rate of rotation of the two cations: it slows down that of **3** and speeds up that of **4**, as seen in Figures 1 and 2. This difference is not caused by the change in solvent properties, because **3**·TFMSA$^-$ in TFA (Figure 1c) behaves exactly like **3**·TFMSA$^-$ in excess TFMSA. The variation in tumbling rate correlates with the difference in basicity of the anions. This correlation suggests that the cation in the trifluoromethanesulfonate salt is fully solvated (free ion in solution), but it is predominantly or fully ion-paired in the trifluoroacetate salt. The ion pairing hinders the rotation of **3** and aids the rotation of **4**, an effect that can be rationalized on the basis of the position of the anion relative to the axis of rotation responsible for relaxation.

The rotation of **3** and **4** can be described with the use of three axes, as shown schematically in Figure 3. Note that the origin of the axes (taken to be the center of mass) is not the same for the two ions. An examination of the longitudinal relaxation times for the carbon atoms, T_{1C}, indicates that rotation about the C_2 axis (x), or for that matter about any axis connecting two atoms located "para" to each other, does not contribute to the relaxation. Thus, rotation about the z axis (perpendicular to the plane of the ring) is likely to be the most effective for NMR relaxation. For the case of strong hydrogen bonding, the anion paired with **3** should be aligned along the x axis.[15] Two different scenarios can be envisioned for rotation about the z axis (perpendicular to the plane) and even about the y axis (in plane). In one limit, the cation and anion move as a unit. Because of its size and shape, this rotor must displace a significantly larger solvent volume upon rotation, leading to more viscous drag. In the other limit, the rotation breaks the interaction between cation and anion, possibly concertedly with a hydron transfer to the anion from an adjacent solvent molecule, such that the rotation of the cation is accompanied by a circular movement of hydrons in the opposite direction. The breaking of the ion pair acts as a slow, or rate-limiting, step in this mechanism. Consequently, ion pairing should slow the rotation of **3**, in agreement with the results shown in Figure 1 and Table 2.

A more quantitative and subtle analysis is required to understand the opposite behavior of **3** and **4** when the solvent changes from TFMSA to TFA. Table 3 provides both stick and slip hydrodynamic boundary condition calculations for the rotational correlation times of solutes **3** and **4** and their ion pairs. These correlation times were obtained using an asymmetric rotor model for the solute diffusion tensor and assuming that the frictional coupling with the solvent can be described by hydrodynamics. The two limiting cases of slip and stick hydrodynamic boundary conditions are presented.[24,40] The table reveals a significant difference between the slip and stick boundary conditions, ranging from a factor of 4 to a factor of 30. Whereas it is fairly well established that small nonpolar molecules in a nonpolar solvent are described by slip boundary conditions or something weaker, the boundary conditions for charged or polar solutes in polar solvents can range from the slip limit to the stick limit (and beyond). Because of difficulties in determining q from eq 5, it is not possible to confirm directly which boundary condition is operative.

TABLE 3: Rotational Correlation Times[a] from Hydrodynamic Boundary Condition Calculations

ion or ion pair	τ_c/η (ps/cP)	τ_c/η (ps/cP)	τ_c/τ_c (ip) stick	τ_c/τ_c (ip) slip	τ_c(TFMSA)/ τ_c(TFA)[b]
3[c]	26	7	–	–	–
3ip (side)[d]	60	13	2.3	1.9	>1
3ip (top)[e]	47	1	1.8	0.14	>1
4[c]	83	4	–	–	–
4ip (side)[d]	127	6	1.5	1.5	<1
4ip (top)[e]	118	4	1.4	1.0	<1

[a] Rotational correlation times: τ_c. [b] From NMR relaxation times. [c] Fully solvated ion. [d] Cation in an ion pair, with the anion in the plane of the ring (hydrogen-bonded). [e] Cation in an ion pair, with the anion perpendicular to the ring.

Comparison of the stick relaxation times for the different systems is particularly useful, because it reflects the impact of molecular size on the relaxation time. The faster rotation of pyridinium, **3**, than of di-*tert*-butylpyridinium, **4**, is reproduced, both for the free ions and for the ion pairs. For **3**, the correlation time increases upon ion pairing for either orientation of the anion. The increase for the orientation with the anion coordinated above the ring is smaller than that for the orientation with the anion in the plane of the ring, which reflects the more spherical shape of the former ion pair; thus, it displaces a smaller volume of fluid and experiences less viscous drag. For the case of di-*tert*-butylpyridinium, **4**, the free cation has a relaxation time that is similar to that of the ion pair. As with the case of **3**, one finds that the more spherical ion pair relaxes more rapidly than the more elongated complex, but the differences are less important for **4**. These shape effects are also identifiable for the slip boundary condition calculations, which do not, however, reflect the differences between **3** and **4** that were observed in both solutions. The experimentally observed trends in the correlation time τ_c between TFA and TFMSA are reproduced for the expected configuration of the hydrogen-bonded ion pair of **3** (anion on the x axis), but they are somewhat closer to the prediction for the configuration with the anion at the top of the ring for the ion pair of **4**.

The existence of hydrogen bonding at the nitrogen-bonded hydrogen atom of **4**, which would place the anion along the x axis, is unlikely in light of the absence of that interaction in the free base,[20] as discussed above. The hydrogen bonding at the nitrogen in **2** requires a distortion of the *tert*-butyl groups, which appears to require more energy than the hydrogen-bond formation liberates. It was noted, however, that breaking of the hydrogen bonds of the donor (e.g., water[26]) with the solvent molecules must also occur, so that only the difference in energy between the two hydrogen bonds is available. To provide a more stringent test of the availability of the nitrogen atom in **2** for

hydrogen bonding, we examined the interaction of **2** (0.07 M solution) with water in methyl *tert*-butyl ether (MTBE) as the solvent, because the steric hindrance reduces the energy of hydrogen-bond formation between water and this solvent. The nitrogen in **2** resonates at a frequency 0.72 ppm lower (negative δ) in MTBE than that in a 0.063 M solution in hexane. The addition of up to 13 equiv of water to the MTBE solution does not affect the relative chemical shift of **2**: δ −0.74 ppm, in this case. This result shows that hydrogen-bond formation at nitrogen with water as the donor does not occur. For the interaction of **4** with the anion, the stronger electrostatic interaction is balanced by the greater steric requirements of the anion.

The analysis of frictional coupling by hydrodynamic boundary condition calculations presented above, does not include electrostatic interactions between the solute and the solvent. Numerous studies have shown that such interactions are significant, especially for cations in polar solvents.[41] The difference between the electrostatic interactions is probably responsible for the difference between the ratio T_{1N}(**3**)/T_{1N}(**4**) (about 20 in TFMSA) and the calculated ratio τ_c(**4**)/τ_c(**3**) (3.2, from Table 3). Earlier work by one of us has shown, however, that the relaxation of ion pairs is well described by hydrodynamics.[42] The origin of this effect comes from the charges being shielded from the solvent by the rest of the molecular ions. Therefore, we expect that the electrostatic contribution to the frictional coupling will be smaller for the ion pair species than for the fully solvated ions in TFMSA. This reduction in the electrostatic friction should also contribute to the shorter rotational correlation time τ_c for **4** in TFA, as compared to TFMSA.

It can also be observed that, for a location above the ring, the anion interacts electrostatically with positively charged hydrogen atoms in the *tert*-butyl groups, as also found for ion pairs of carbocations.[43] An estimation of the charge distribution for the structure of **4**, obtained from geometry optimization at the B3LYP/6-31G* level, is presented in the second column of Table 4. It shows the existence of four positively charged hydrogen atoms, two in each *tert*-butyl group, oriented away from the ring, on each side (axial hydrogens). The same calculation shows that there is a significant concentration of positive charge in the six hydrogen atoms of the substituents situated on the sides of the ring (equatorial hydrogens). It is the interaction of these hydrogens and the ring hydrogens (Hβ and Hγ) with the dipoles of solvent molecules that slows down the rotation about the *z* axis of the free ion **4** (in TFMSA solution) beyond what is expected from the difference in size between **3** and **4**. Moreover, a calculation of the charge distribution in **4** ion-paired with two model anions, hydride and fluoride, placed 4 Å above the ring, shows that ion pairing pushes negative charge from the axial hydrogens facing the anion (proximal hydrogens) onto the equatorial hydrogens and the ring hydrogens. The axial hydrogens on the other side of the ring (distal hydrogens) also have their positive charge reduced by ion pairing. The results are shown in the third and fourth columns of Table 4. Therefore, the electrostatic friction[44] that slows the rotation of **4** is reduced upon ion pairing. The tumbling correlation time, τ_c, decreases, and the NMR longitudinal relaxation time, T_1, increases, as experimentally observed. Some puckering of the ring also occurs upon ion pairing of **4**; however, the reduction in diameter and the consequent increase in sphericity of the ion pair is small, and the effect on the tumbling rate, albeit in the right direction, should be less important than the effect of the charge redistribution.[45]

TABLE 4: B3LYP/6-31G* Charge Distribution in DTBPH$^+$ (4) and Its Ion Pairs[a]

		4	**4**·H$^-$	**4**·F$^-$
1	N	−0.684	−0.699	−0.658
2	Cα	0.442	0.409	0.416
3	Cα	0.442	0.409	0.416
4	Cβ	−0.214	−0.207	−0.205
5	Cβ	−0.214	−0.207	−0.205
6	Cγ	−0.062	−0.112	−0.085
7	(N)H	0.372	0.360	0.379
8	Hβ	0.204	0.154	0.171
9	Hβ	0.204	0.154	0.171
10	Hγ	0.211	0.150	0.171
11	C(sp^3, quat)	−0.024	0.002	−0.001
12	C(sp^3, quat)	−0.024	0.002	−0.001
13	C	−0.470	−0.460	−0.461
14	C	−0.456	−0.435	−0.436
15	C	−0.456	−0.486	−0.534
16	C	−0.470	−0.460	−0.461
17	C	−0.456	−0.435	−0.436
18	C	−0.456	−0.486	−0.534
19	H(e)[b]	0.186	0.153	0.164
20	H(a, p)[b]	0.170	0.176	0.183
21	H(a, d)[b]	0.170	0.142	0.135
22	H(e)[b]	0.194	0.157	0.166
23	H(a, d)[b]	0.178	0.150	0.145
24	H	0.143	0.140	0.141
25	H(e)[b]	0.194	0.151	0.147
26	H	0.143	0.126	0.116
27	H(a, p)[b]	0.178	0.204	0.254
28	H(e)[b]	0.186	0.153	0.164
29	H(a, p)[b]	0.170	0.176	0.183
30	H(a, d)[b]	0.170	0.142	0.135
31	H(e)[b]	0.194	0.157	0.166
32	H(a, d)[b]	0.178	0.150	0.145
33	H	0.143	0.140	0.141
34	H(e)[b]	0.194	0.151	0.147
35	H	0.143	0.126	0.116
36	H(a, p)[b]	0.178	0.204	0.254

[a] Mulliken population analysis on the structure optimized at the B3LYP/6-31G* level. In the ion pair, the anion is held 4.0 Å above the ring. [b] e = equatorial hydrogens, a = axial hydrogens, p = proximal hydrogens (close to the anion), and d = distal hydrogens (on the other side of the ring than the anion).

The difference in position of the anion relative to the cation in the ion pairs of **3** and **4** is significant for their chemisorption on solid acids. Because ions on solid surfaces are always formed as intimate ion pairs,[14] pyridine will be adsorbed to form **3** with the N−H$^+$ group facing the surface (sidewise), whereas **4**, which results from the hydronation of **2**, will be oriented with the ring facing the surface (flatwise). Thus, **4** will occupy even more space on the surface than formerly believed. As another consequence, the level of hydronation of **2** will depend not only upon the intrinsic strength of the acid sites but also on the curvature of the surface, which will determine how close the cation **4** can come to the anion on the surface.[46] We find, therefore, another complicating factor in the evaluation of acid strength of solids with probe bases, in addition to the relative distance and position of acid sites in pores identified in a study of the hydronation of water.[47]

Acknowledgment. Discussions with Prof. Edwin D. Becker, Prof. Avelino Corma, and Prof. Thomas C. Farrar are gratefully acknowledged. This work was supported by grants (CTS-9812704, strong acid catalysis; CTS-9413698, purchase of a DMX300 NMR instrument) from the U.S. National Science Foundation and a grant of supercomputer time (CHE-980021N) from the National Center for Supercomputing Applications at the centers in Urbana, IL, and Lexington, KY.

References and Notes

(1) Address questions on the hydrodynamic boundary condition calculations to this author.

(2) Mills, G. A.; Boedeker, E. R.; Oblad, A. G. *J. Am. Chem. Soc*. **1950**, *72*, 1554.

(3) (a) Peri, J. B.; Hamman, R. B. *J. Phys. Chem*. **1960**, *64*, 1526. (b) Parry, E. P. *J. Catal*. **1963**, *2*, 371. (c) For a review, see: Paukshtis, E. A.; Yurchenko, E. N. *Russ. Chem. Rev*. **1983**, *52*, 242.

(4) Auroux, A.; Wierzchowski, P.; Gravelle, P. *Thermochim. Acta* **1979**, *32*, 165.

(5) Freude, D.; Pfeifer, H.; Ploss, W.; Staudte, B. *J. Mol. Catal*. **1981**, *12*, 1.

(6) (a) Gay, I. D.; Liang, S. *J. Catal*. **1976**, *44*, 306. (b) Rauscher, H.-J.; Michel, D.; Deininger, D.; Geschke, D. *J. Mol. Catal*. **1980**, *9*, 369. (c) Dawson, W. H.; Kaiser, S. W.; Ellis, P. D.; Inners, R. R. *J. Phys. Chem*. **1982**, *86*, 867.

(7) (a) Maciel, G. E.; Haw, J. F.; Chuang, I.-S.; Hawkins, B. L.; Early, T. A.; McKay, D. R.; Petrakis, L. *J. Am. Chem. Soc*. **1983**, *105*, 5529. (b) Ripmeester, J. A. *J. Am. Chem. Soc*. **1983**, *105*, 2925.

(8) Lercher, J. A.; Rumplmayr, G.; Lebok, J.; Ritter, G. *Stud. Surf. Sci. Catal*. **1985**, *7*, 1669.

(9) (a) Fărcaşiu, D.; Ghenciu, A. *J. Am. Chem. Soc*. **1993**, *115*, 10901. (b) Sikabwe, E. C.; Coelho, M. A.; Resasco, D. E.; White, R. L. *Catal. Lett*. **1995**, *34*, 23. (c) Srinivasan, R.; Keogh, R. A.; Ghenciu, A.; Fărcaşiu, D.; Davis, B. H. *J. Catal*. **1996**, *158*, 502.

(10) Benesi, H. A. *J. Catal*. **1973**, *28*, 176.

(11) (a) Jacobs, P. A.; Heylen, C. F. *J. Catal*. **1974**, *34*, 267. (b) Corma, A.; Rodellas, C.; Fornet, V. *J. Catal*. **1984**, *88*, 374.

(12) (a) Dewing, J.; Monks, G. T.; Youll, B. T. *J. Catal*. **1976**, *44*, 226. (b) Knözinger, H.; Krietenbrink, H.; Ratnasamy, P. *J. Catal*. **1977**, *48*, 436. (c) Matulewicz, E. R. A.; Kerkhof, F. P. J.; Moulijn, J. A. *J. Colloid Interface Sci*. **1980**, *77*, 110. (d) Miyata, H.; Moffat, J. B. *J. Catal*. **1980**, *62*, 357.

(13) (a) Keskinen, K. M.; Pakkanen, T. T.; Raulo, P.; Ruotsalainen, M.; Sarv, P.; Titta, M. *Stud. Surf. Sci. Catal.* **1994**, *84*, 875. (b) Corma, A.; Fornés, V.; Forni, L.; Márques, F.; Martínez-Triguero, J.; Moscotti, D. *J. Catal*. **1998**, *179*, 451.

(14) (a) Fărcaşiu, D.; Ghenciu, A.; Miller, G. *J. Catal.* **1992**, *134*, 118. (b) Fărcaşiu, D.; Ghenciu, A.; Li, J. Q. *J. Catal.* **1996**, *158*, 116. (c) Ghenciu, A.; Fărcaşiu, D. *J. Mol. Catal. A* **1996**, *109*, 273. (d) Fărcaşiu, D.; Ghenciu, A. *Prog. Nucl. Magn. Reson. Spectrosc.* **1996**, *29*, 129.

(15) (a) Petrakis, L.; Kiviat, F. E. *J. Phys. Chem*. **1976**, *80*, 606. (b) Cardona-Martinez, N.; Dumesic, J. A. *J. Catal*. **1990**, *125*, 427.

(16) (a) Brown, H. C.; Kanner, B. *J. Am. Chem. Soc*. **1953**, *75*, 3865. (b) Brown, H. C.; Kanner, B. *J. Am. Chem. Soc*. **1966**, *88*, 986. (c) McDaniel, D. H.; Ozcan, M. *J. Org. Chem*. **1968**, *33*, 1922. (d) Arnett, E. M.; Chawla, B. *J. Am. Chem. Soc.* **1978**, *100*, 217. (e) Arnett, E. M.; Chawla, B. *J. Am. Chem. Soc*. **1979**, *101*, 7141. (f) Benoit, R. L.; Fréchette, M.; Lefebvre, D. *Can. J. Chem*. **1988**, *66*, 1159.

(17) Condon, F. E. *J. Am. Chem. Soc*. **1965**, *87*, 4494.

(18) Hopkins, H. P., Jr.; Jahagirdar, D. V.; Moulik, P. S.; Aue, D. H.; Webb, H. M.; Davidson, W. R.; Pedley, M. D. *J. Am. Chem. Soc*. **1984**, *106*, 4341.

(19) Chardin, A.; Laurence, C.; Berthelot, M. *J. Chem. Res., Synop.* **1996**, 332.

(20) Fărcaşiu, D.; Lezcano, M.; Vinslava, A. *New J. Chem*. **2000**, *24*, 199.

(21) Frisch, M. J.; Trucks, G. W.; Schlegel, H. B.; Scuseria, G. E.; Robb, M. A.; Cheeseman, J. R.; Zakrzewski, V. G.; Montgomery, J. A., Jr.; Stratmann, R. E.; Burant, J. C.; Daprich, S.; Millam, J. M.; Daniels, A. D.; Kudin, K. N.; Strain, M. C.; Farkas, O.; Tomasi, J.; Barone, V.; Cossi, M.; Cammi, R.; Mennucci, B.; Pomelli, C.; Adamo, C.; Clifford, S.; Ochterski, J.; Petersson, G. A.; Ayala, P. Y.; Cui, Q.; Morokuma, K.; Malick, D. K.; Rabuck, A. D.; Raghavachari, K.; Foresman, J. B.; Cioslowski, J.; Ortiz, J. V.; Stefanov, B. B.; Liu, G.; Liashenko, P.; Piskorz, P.; Komaromi, I.; Gomperts, R.; Martin, R. L.; Fox, D. J.; Keith, T.; Al-Laham, M. A.; Peng, C. Y.; Nanayakkara, A.; Gonzalez, C.; Challacombe, M.; Gill, P. M. W.; Johnson, B. G.; Chen, W.; Wong, M. W.; Andres, J. L.; Head-Gordon, M.; Replogle, E. S.; Pople, J. A. *Gaussian 98, revision A.1*; Gaussian, Inc.: Pittsburgh, PA, 1998.

(22) (a) Hohenberg, P.; Kohn, W. *Phys. Rev.* **1964**, *136*, B864. (b) Kohn, W.; Sham, L. J. *Phys. Rev.* **1965**, *140*, A1133. (c) Parr, R. G.; Yang, W. *Density-Functional Theory of Atoms and Molecules*; Oxford University Press: Oxford, U.K., 1989.

(23) (a) Becke, A. D. *J. Chem. Phys.* **1993**, *98*, 5648. (b) Lee, C.; Yang, W.; Parr, R. G. *Phys. Rev.* **1988**, *B37*, 78564.

(24) (a) Hartman, R. S.; Konitsky, W. M.; Waldeck, D. H.; Chang, Y. J.; Castner, E. W., Jr. *J. Chem. Phys.* **1997**, *106*, 7920. (b) Fleming, G. R. *Chemical Applications of Ultrafast Spectroscopy*; Oxford University Press: New York, 1986.

(25) Currently part of SPSS, Inc. (http://www.spss.com/software/science/SigmaPlot/).

(26) Preliminary communication: Fărcaşiu, D.; Lezcano, M. *Phys. Chem. Chem. Phys*. **1999**, *1*, 3753.

(27) Baldeschweiler, J. D.; Randall, E. W. *Proc. Chem. Soc., London* **1961**, 303. Figures 1 and 2 in that paper were, obviously, interchanged.

(28) Allen, M.; Roberts, J. D. *J. Org. Chem*. **1980**, *45*, 130.

(29) Smirnov, S. N.; Golubev, N. S.; Denisov, G. S.; Benedict, H.; Schach-Mohammedi, P.; Limbach, H. *J. Am. Chem. Soc*. **1996**, *118*, 4094.

(30) Witanowski, M.; Stefaniak, L.; Webb, G. A. *Annual Reports on NMR Spectroscopy*; Webb, G. A., Ed.; Academic Press: London, 1993; Vol. 25, p 70.

(31) (a) Watanabe, S.; Ando, I. *J. Mol. Struct*. **1981**, *77*, 283. (b) Witanowski, M.; Stefaniak, L.; Webb, G. A. *Annual Reports on NMR Spectroscopy*; Webb, G. A., Ed.; Academic Press: London, 1986; Vol. 18, p 192 and Table 130.

(32) (a) Grunwald, E.; Ralph, E. K. *Acc. Chem. Res*. **1971**, *4*, 107. (b) Grunwald, E.; Eustace, D. In *Proton-Transfer Reactions*; Caldin, E. F., Gold, V., Eds.; Chapman and Hall: London, 1975; Chapter 4. (c) Gold, V.; Lee, R. A. *J. Chem. Soc., Chem. Commun*. **1984**, 1032.

(33) Roberts, J. D. *J. Am. Chem. Soc*. **1956**, *78*, 4495.

(34) Ogg, R. A. *Faraday Discuss.* **1954**, *17*, 215.

(35) Shoolery, J. N. Cited (as ref 2) in ref 33.

(36) (a) Pople, J. A. *Mol. Phys*. **1958**, *1*, 168. (b) Suzuki, M.; Kubo, R. *Mol. Phys*. **1964**, *7*, 201. (c) Witanowski, M.; Webb, G. A. *Annual Reports on NMR Spectroscopy*; Mooney, E. F., Ed.; Academic Press: London, 1972; Vol. 5A, p 414.

(37) Becker, E. D. *High-Resolution NMR. Theory and Chemical Applications*, 2nd ed.; Academic Press: Orlando, FL, 1980; (a) p 192, (b) pp 186−7, (c) pp 188−9.

(38) Vold, R. D.; Waugh, J. S.; Klein, M. P.; Phelps, D. E. *J. Chem. Phys*. **1968**, *48*, 3831.

(39) Gerothanassis, I. P.; Tsanaktsidis, C. G. *Concepts Magn. Reson.* **1996**, *8*, 63.

(40) Huntress, W. T. *Adv. Magn. Reson*. **1970**, *4*, 1.

(41) (a) Balabai, N.; Sukharevsky, A.; Read, I.; Strazisar, B.; Kurnikova, M.; Hartman, R. S.; Coalson, R. D.; Waldeck, D. H. *J. Mol. Liq.* **1998**, *77*, 37. (b) Hartman, R. S.; Alavi, D. S.; Waldeck, D. H. *Isr. J. Chem*. **1993**, *33*, 157. (c) Alavi, D. S.; Waldeck, D. H. *Understanding Chemical Reactivity*; Kluwer Academic Publishers: Dordrecht, The Netherlands, 1994; pp 249−65.

(42) (a) Balabai, N.; Kurnikova, M.; Coalson, R. D.; Waldeck, D. H. *J. Am. Chem. Soc.* **1998**, *120*, 7944. (b) Balabai, N.; Waldeck, D. H. *J. Phys. Chem.* **1997**, *101*, 2339. (c) Hartman, R. S.; Konitsky, W.; Waldeck, D. H. *J. Am. Chem. Soc*. **1993**, *115*, 9692.

(43) (a) Fărcaşiu, D.; Lukinskas, P. *J. Phys. Chem. A* **1998**, *102*, 10436. (b) Fărcaşiu, D.; Hâncu, D. *J. Am. Chem. Soc*. **1999**, *121*, 7173 and other papers in the series.

(44) The term electrostatic friction describes the interaction of points of charge in the molecule or ion (atoms carrying electrical charges) with ions or dipoles around it, whereas the term dielectric friction describes the interaction of a particle or ion uniformly charged with a uniform dielectric medium. For the latter, see: (a) Alavi, D. S.; Waldeck, D. H. *J. Chem. Phys*. **1991**, *94*, 6196. (b) Bordes, B.; Coletta, F.; Ferrarini, A.; Gottardi, F.; Nordio, P. L. *Chem. Phys.* **1998**, *231*, 51.

(45) The position of the anion can, in principle, be determined by interionic nOe experiments, but the tertiary butyl proton signal is the only convenient signal of **4** to be irradiated for this purpose and it could not distinguish between the anion in the plane of the ring or above it.

(46) Realization of this point came from a discussion with A. Corma.

(47) Fărcaşiu, D.; Lukinskas, P., submitted for publication.